Available online at www.sciencedirect.com

SCIENCE DIRECT

Virology 336 (2005) 274 – 290

VIROLOGY

www.elsevier.com/locate/yviro

African green monkey kidney Vero cells require de novo protein synthesis for efficient herpes simplex virus 1-dependent apoptosis

Marie L. Nguyen, Rachel M. Kraft, John A. Blaho*

Department of Microbiology, Mount Sinai School of Medicine, One Gustave L. Levy Place, New York, NY 10029, USA

Received 24 January 2005; returned to author for revision 23 February 2005; accepted 9 March 2005
Available online 20 April 2005

Abstract

During HSV-1 infection, IE gene expression triggers apoptosis, but subsequent synthesis of infected cell proteins blocks apoptotic death from ensuing. This "HSV-1-dependent" apoptosis was identified in HEp-2/HeLa cells infected with wild-type HSV-1 in the presence of an inhibitor of protein synthesis or a virus lacking ICP27 {HSV-1(vBSΔ27)}. Unlike HEp-2/HeLa cells, vBSΔ27-infected Vero cells fail to exhibit dramatic apoptotic morphologies at times prior to 24 hpi. Here, we examined the basis of these different apoptotic responses to HSV-1. We found that infected Vero cells take substantially longer than HEp-2/HeLa cells to display membrane blebbing, chromatin condensation, DNA laddering, and PARP cleavage. Vero, but not HEp-2/HeLa, cells required de novo protein synthesis to exhibit efficient HSV-1-dependent apoptosis, which included changes in mitochondrial membrane potential, and these factors were produced prior to 3 hpi. Vero cells infected with recombinant viruses devoid of the ICP27 and ICP4 proteins alone or both the ICP27 and ICP22 proteins were apoptotic. These results indicate a requirement for cellular or other viral protein synthesis in Vero cells and provide insight into cell type differences in HSV-1-dependent apoptosis.

Keywords: Apoptosis; Herpes simplex virus; Vero; HEp-2/HeLa; Protein synthesis

Introduction

Apoptosis is a highly regulated form of cell death that is common to many physiological and pathological processes (reviewed in Vaux and Strasser, 1996; White, 1996). During apoptosis, a cascade of cysteinyl-aspartate-kinases (caspases) is activated (reviewed in Salvesen and Dixit, 1997; Villa et al., 1997). Initiator caspases activate effector caspases that allow for the progression of apoptosis by cleaving many cellular enzymes important for cell maintenance, e.g., a DNA repair enzyme, poly(ADP-ribose)polymerase (PARP), and a DNAse inhibitor, DFF-45 (reviewed in Sanfilippo and Blaho, 2003). Ultimately, the destruction of the cell via apoptosis leads to specific morphological changes including chromatin condensation, nucleosomal DNA fragmentation, disruption of mitochondrial membrane potential, and membrane blebbing (Kerr and Harmon, 1991; Kerr et al., 1972; Wyllie et al., 1980).

Although much of the disease associated with herpes simplex virus 1 (HSV-1) infection is due to the lysis of infected cells, a subset of HSV-1-induced pathologies has been reported to contain an apoptotic component. In one study, Perkins et al. found that tissue sections from HSV-associated acute focal encephalitis contained cells with active caspase 3 and cleaved PARP (Perkins et al., 2003). They also found that HSV-1 infection increased the levels of these apoptotic markers in hippocampal cultures. Additionally, investigators have reported the presence of apoptotic cells in mouse (Zheng et al., 2001) and rabbit (Wilson et al., 1997) eyes infected with HSV-1. These findings suggest that modulation of apoptosis by HSV-1 might be important in the development of herpetic disease.

HSV-1 first triggers HSV-1-dependent apoptosis and then blocks apoptosis in infected cells in culture. Koyama et al. were the first to identify that HEp-2/HeLa cells infected

* Corresponding author. Fax: +1 212 534 1684.
E-mail address: john.blaho@mssm.edu (J.A. Blaho).

0042-6822/$ - see front matter © 2005 Elsevier Inc. All rights reserved.
doi:10.1016/j.virol.2005.03.026

with wild-type HSV-1 in the presence of the protein synthesis inhibitor, cycloheximide (CHX), die by apoptosis (Koyama and Adachi, 1997). This indicated that HSV-1 was able to trigger apoptosis in the absence of de novo viral protein synthesis. Our laboratory demonstrated that cells infected with UV-inactivated HSV-1 in the absence or presence of CHX failed to die by apoptosis. Since UV-irradiated viruses are capable of entry, deenvelopment, and nuclear translocation, these activities are insufficient to trigger apoptosis in infected cells (Aubert and Blaho, 1999; Aubert et al., 1999; Sanfilippo et al., 2004). Recently, we determined that the HSV apoptotic trigger requires transcription of immediate early viral genes (Sanfilippo et al., 2004). Additionally, we have found that the addition of CHX prior to 3 h post-infection (hpi), but not after 6 hpi, resulted in apoptosis of HSV-1-infected cells (Aubert et al., 1999). Taken together, these data led us to conclude that HSV-1 triggers apoptosis through a mechanism independent of de novo protein synthesis and that between 3 and 6 hpi infected cell proteins are produced which prevent apoptotic death from ensuing (Aubert and Blaho, 2001; Goodkin et al., 2004).

Several laboratories have identified viral genes which play roles in apoptosis modulation by HSV-1. HSV-1 viral replication is controlled by a coordinated cascade (reviewed in Roizman and Sears, 1996), and transcriptional activation by the IE gene products, especially ICP27 and ICP4, is necessary for expression of the later viral genes and the subsequent production of progeny virions (DeLuca and Schaffer, 1985; DeLuca et al., 1985; Dixon and Schaffer, 1980; Hardwicke et al., 1989; McCarthy et al., 1989; Preston, 1979; Rice and Knipe, 1990; Sacks et al., 1985; Soliman et al., 1997; Watson and Clements, 1980). Infection of cells with a mutant virus defective for both ICP4 and U_S3, *d*120, leads to apoptosis (Galvan et al., 1999; Leopardi and Roizman, 1996; Leopardi et al., 1997). A virus lacking ICP27, vBSΔ27, also causes infected cells to die by apoptosis (Aubert and Blaho, 1999). Furthermore, infection with a series of viruses carrying mutations in ICP27 that were incapable of transactivating early and leaky-late gene expression led to apoptosis of infected cells (Aubert et al., 2001). Infection with replication-defective viruses such as these triggers apoptosis, but infected cell survival factors are not produced, and the cells ultimately die by apoptosis. In support of this conclusion, several other antiapoptotic HSV-1 genes have been identified (Hagglund et al., 2002; Jerome et al., 1999; Leopardi and Roizman, 1996; Perng et al., 2000; Zhou and Roizman, 2002). The above findings led us to propose a model in which there is a balance between the trigger and the preventers of apoptosis during productive HSV-1 infection (Aubert and Blaho, 2001; Goodkin et al., 2004). Maintaining this balance allows productive viral replication, which lyticly kills cells resulting in cytopathic effect (CPE), whose features include cell swelling, nuclear enlargement, marginalization of the cellular chromatin, and cell lysis (Avitabile et al., 1995; Hampar and Elison, 1961; Heeg et al., 1986; Roizman, 1962; Roizman and Roanne, 1964; Roizman and Sears, 1996). When the balance is upset due to a reduction in late viral protein synthesis, e.g., experimentally through the disruption of important IE viral proteins or the addition of CHX, it results in apoptosis of the infected cell.

This model is based primarily on data generated using the human carcinoma HEp-2 cell line (Moore et al., 1955), now known to be a HeLa cell-derived strain (Chen, 1988; Nelson-Rees et al., 1974) and referred to here as HEp-2/HeLa. However, not all cell types display identical apoptotic responses to HSV-1 infection. In our original study describing HSV-1-dependent apoptosis, infected African green monkey kidney Vero cells differed from HEp-2/HeLa cells by their apparent inability to display abundant morphological apoptotic features (Aubert and Blaho, 1999). Similarly, Gautier et al. reported that HSV-1 infected Vero cells do not display an alteration in mitochondrial membrane potential at 1 and 3 hpi (Gautier et al., 2003). These results suggest that Vero cells fail to undergo efficient HSV-1-dependent apoptosis. However, others have reported that Vero cells infected with the HSV-1(*d*120) mutant virus exhibit TUNEL positive staining, DNA laddering, and nuclear changes at or after 24 hpi (Galvan et al., 1999; Leopardi and Roizman, 1996; Leopardi et al., 1997).

This apparent discrepancy among studies led us to specifically compare the HSV-1-dependent apoptosis of Vero and HEp-2/HeLa cells and determine the underlying causes behind these differences. We report the following. Vero cells did exhibit specific apoptotic morphologies following infection with either ICP27- or ICP4-null viruses, but these features took longer to manifest than those of the HEp-2/Hela cells. Vero cells required de novo protein synthesis to undergo efficient HSV-1-dependent apoptosis while HEp-2/HeLa cells did not. The required protein(s) was synthesized prior to 3 hpi in vBSΔ27-infected Vero cells. Viruses deleted for ICP4, ICP27, and ICP22 induced Vero cell apoptosis, implying that either cellular or other viral proteins are needed for this process to occur. These results help to clarify our understanding of the cell type differences in HSV-1-dependent apoptosis.

Results

Vero and HEp-2/HeLa cells displayed temporal and qualitative differences in the appearance of HSV-1-dependent apoptotic morphologies

The first goal of this study was to carefully compare HSV-1-dependent apoptosis in Vero and HEp-2/HeLa cells. Among the evidence in support of Vero cells being susceptible to HSV-1-dependent apoptosis was that DNA laddering was observed at 24 and 30 h following infection with the ICP4 and U_S3 null virus, *d*120 (Galvan et al., 1999; Leopardi and Roizman, 1996; Leopardi et al., 1997). Our

laboratory reported that Vero cells infected with the ICP27-null virus, vBSΔ27, fail to display DNA laddering at 15 hpi, while vBSΔ27-infected HEp-2/HeLa cells exhibit maximum DNA laddering at 12 hpi (Aubert and Blaho, 1999). The fact that DNA laddering was detected by others later in Vero cells than we observed in HEp-2/HeLa cells suggests that HSV-1-dependent apoptosis is slower in Vero cells. To test this idea, a time-course experiment was performed with both cell lines. HEp-2/HeLa and Vero cells were infected with HSV-1(KOS1.1) or vBSΔ27 virus at a multiplicity of infection (MOI) of 10 in the presence and absence of CHX, and morphological changes were assessed by phase-contrast microscopy at 12, 24, and 36 hpi (Fig. 1).

As expected, HSV-1(KOS1.1) infection in the absence of CHX led to increased cell size, rounded morphologies (Fig. 1), and marginalization of chromatin in the nuclei (data not shown) of both HEp-2/HeLa and Vero cells. These characteristics are indicative of CPE, which accompanies productive HSV-1 infection. CPE was evident at 12 hpi and reached a maximum by 24 hpi in both cell lines. Consistent with previous reports from our laboratory (Aubert and Blaho, 1999; Aubert et al., 1999), HEp-2/HeLa cells infected with vBSΔ27 exhibited apoptotic morphologies including a reduced overall cell size and irregular membranes. This phenotype was present as early as 12 hpi and reached its maximum at 24 hpi. In contrast, vBSΔ27-infected Vero cells failed to exhibit similar morphologies at 12 hpi. At 24 hpi, approximately half of the vBSΔ27-infected Vero cells appeared smaller and irregularly-shaped compared to mock-infected cells, suggestive of apoptosis in these cells. Although the number of Vero cells displaying altered morphologies increased slightly from 24 to 36 hpi, they never reached the level displayed by HEp-2/HeLa cells. These results

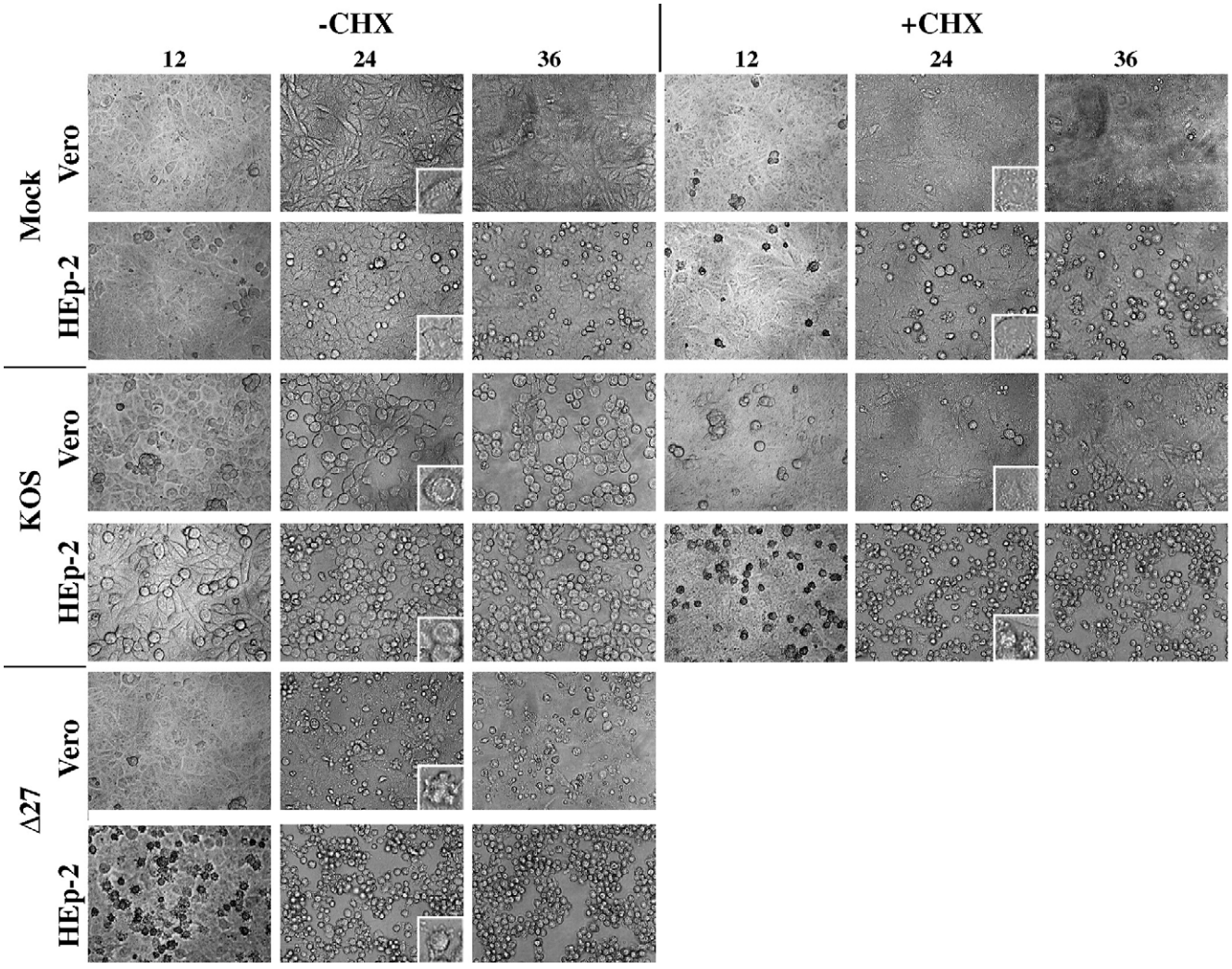

Fig. 1. Morphological assessment of HEp-2/HeLa and Vero cells during HSV-1-dependent apoptosis. Vero and HEp-2/HeLa cells were infected with wild-type HSV-1(KOS1.1) in the presence (+) or absence (−) of 10 μg/ml CHX or ICP27-null virus, vBSΔ27, at an MOI of 10. Cells were visualized by phase contrast light microscopy (magnification, ×40) and photographed at 12, 24, and 36 hpi. Insets within the photos of the 24 hpi time points correspond to enlarged images of representative cells from each photo.

indicate that although Vero cells do exhibit morphologies similar to apoptotic cells when infected with vBSΔ27, they do so to a much lower extent and with slower kinetics than HEp-2/HeLa cells.

A more prominent distinction between the two cell lines was revealed when protein synthesis was inhibited during infection. Treatment with CHX alone induced a low-level, background amount of apoptosis in mock-infected HEp-2/HeLa cells, probably due to the depletion of preexisting cellular survival factors that were not replenished when protein synthesis was blocked. As expected, apoptosis was drastically increased in KOS plus CHX-treated HEp-2/HeLa cells compared to those only infected with KOS or treated with CHX alone at all time points. In contrast, CHX-treated Vero cells infected with KOS failed to display apoptosis-like morphologies at 12 and 24 hpi. At 36 hpi, a small number of the KOS plus CHX-infected Vero cells seemed to display features of apoptosis, but this did not reach the extent of the morphological changes observed with the vBSΔ27-infected Vero cells.

This finding was quite unexpected. Unlike our results with HEp-2/HeLa cells, there seemed to be some distinction between these two treatments which allowed for HSV-1-dependent apoptosis-like morphological changes of Vero cells in one case (vBSΔ27) but not the other (KOS plus CHX). One major difference is that cellular and some viral protein synthesis likely occurred during vBSΔ27, but not KOS plus CHX infection.

De novo protein synthesis was required for efficient HSV-1-dependent apoptosis in Vero cells

We next set out to test if infected Vero cells displayed other signs of apoptosis and to determine whether proteins synthesized during vBSΔ27 infection might facilitate HSV-1-dependent apoptosis in Vero cells. Four sets of experiments were performed. Since PARP cleavage and chromatin condensation are evident in cells undergoing HSV-1-dependent apoptosis, but not cells dying via CPE (Aubert and Blaho, 1999; Aubert et al., 1999, 2001), we initially used these assays to quantitatively assess apoptosis in infected Vero cells. In the first series, we determined whether inhibition of protein synthesis suppressed HSV-1-dependent PARP cleavage in Vero cells. Vero and HEp-2/HeLa cells were infected with HSV-1(KOS1.1) or vBSΔ27 at an MOI of 5 in the presence or absence of CHX. As an additional positive control for HSV-1-dependent apoptosis (Aubert and Blaho, 2003), we also used a recombinant virus defective for the immediate early protein ICP4 (also termed IE3), CgalΔ3. At 12 and 24 hpi, infected cells were harvested, whole cell proteins were extracted, and PARP cleavage, as well as the presence of ICP27 and TK viral proteins, was assessed by immunoblotting (Fig. 2) as described in Materials and methods.

ICP27 was found in cells infected with HSV-1(KOS1.1) and CgalΔ3, but not vBSΔ27 (lanes 3–6 and 10–12). In Vero cells, TK was present at approximately the same levels

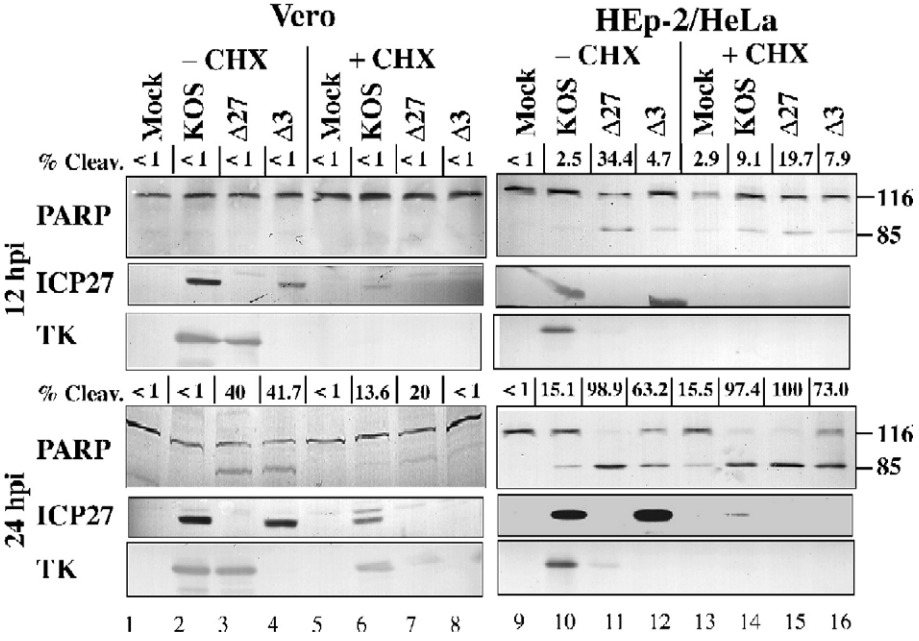

Fig. 2. PARP cleavage of infected cells in the presence and absence of de novo protein synthesis. Vero and HEp-2/HeLa cells were infected with HSV-1(KOS1.1), vBSΔ27, or the ICP4 null virus, CgalΔ3, in the presence (+) or absence (−) of 10 μg/ml CHX as described in Materials and methods. At 12 and 24 hpi, the cells were scraped into the media, collected by centrifugation, and subjected to whole cell protein extraction. 50 μg of protein was used for immunoblot analysis with anti-PARP and anti-ICP27 monoclonal antibodies and anti-thymidine kinase (TK) polyclonal antibody. The migration of the 116,000 molecular weight uncleaved (116) and 85,000 molecular weight cleaved product (85) is indicated in the right margin. NIH image was used to quantify the % PARP cleavage (% cleav.) as described in Materials and methods.

in the lysates of cells infected with HSV-1(KOS1.1) and vBSΔ27, but absent in lysates from cells infected with CgalΔ3 (compare lane 4 with 2 and 3). In vBSΔ27-infected HEp-2 cells, TK was detected at 24, but not 12 hpi (lane 11). This result is consistent with our previous studies indicating that viral proteins accumulate to higher levels in nonhuman cells than in human cells (Aubert and Blaho, 1999; O' Toole et al., 2003). Treatment of the infected cells with CHX greatly reduced the synthesis of all of the viral proteins tested (lanes 6–8 and 14–16). These results confirm that the HEp-2 and Vero cells were similarly infected in this experiment and indicate that CHX treatment resulted in the reduction of viral protein synthesis.

At 12 hpi, PARP cleavage was detectable in lysates from HEp-2/HeLa cells infected with vBSΔ27 (34%) and KOS plus CHX (9%) (Fig. 2, lanes 11 and 14). Less than 3% PARP cleavage was observed in the mock, mock plus CHX, and HSV-1(KOS1.1)-infected HEp-2/HeLa cell lysates (lanes 9, 10, and 13), as well as in all of the Vero cell lysates (lanes 1–9) at this time point. At 24 hpi, mock-infected Vero cells plus CHX displayed <1% PARP cleavage (Fig. 2, lane 5) while similarly treated HEp-2/HeLa cells showed 16% (lane 10). At this time point, PARP was cleaved in the lysates of HEp-2/HeLa cells infected with vBSΔ27 or CgalΔ3, 99% and 63%, respectively (lanes 11 and 12). The presence of CHX did not reduce the level of PARP cleavage in HEp-2/HeLa cells infected with ICP27 (100%) or ICP4 (73%) deletion viruses (compare lanes 15 and 16 with 11 and 12). KOS plus CHX-treated HEp-2/HeLa cells displayed almost complete PARP cleavage (97%) at 24 hpi (lane 14). In contrast, PARP cleavage was only 14% in the lysates of Vero cells infected with KOS plus CHX (lane 6). At this time point, the lysates of vBSΔ27- or CgalΔ3-infected Vero cells without CHX exhibited substantial (40% and 42%) PARP cleavage (compare lanes 3 and 4). The finding that CgalΔ3-infected Vero cells demonstrate apoptotic features suggests that Vero cells are generally sensitive to HSV-1-triggered apoptosis and these observations are not peculiar to vBSΔ27 infection. The presence of CHX reduced PARP cleavage in vBSΔ27-infected Vero cells from 40% to 20% (lanes 3 and 7) and abrogated (42% to <1%) its cleavage in CgalΔ3-infected cells (compare lanes 4 and 8). The reduction of apoptosis during vBSΔ27 plus CHX infection was comparable to that of KOS plus CHX (20% and 14%, respectively). That the level of apoptosis in CgalΔ3 plus CHX-infected cells was less than these values likely reflects parental strain differences (Aubert and Blaho, 2001; Goodkin et al., 2004). This particular experiment has been repeated more than five times (data not shown and additional data later in this study). CHX treatment in vBSΔ27-infected Vero cells reproducibly led to between a 2- and 5-fold reduction in PARP cleavage in each instance. From these results, we conclude that de novo protein synthesis is required for efficient HSV-1-dependent PARP cleavage in Vero cells.

In the second series of experiments, we assessed the role of protein synthesis in HSV-1-dependent chromatin condensation. Vero and HEp-2/HeLa cells were infected in triplicate with HSV-1(KOS1.1) and vBSΔ27 at an MOI of 5 in the presence or absence of CHX. At 24 hpi, Hoechst dye was added to the media and 2–3 random microscopic (40×) fields per replicate were digitally captured. Representative images are shown in Fig. 3A. The percentage of nuclei with condensed chromatin (greater than 400 total cells analyzed per treatment group) was assessed for each microscopic field as described in Materials and methods. A statistical analysis of the data was performed using Student's t test. The percentage of nuclei containing condensed chromatin is presented in Fig. 3B.

34 ± 4% of KOS plus CHX-infected HEp-2/HeLa cells displayed chromatin condensation. In contrast, Vero cells infected with KOS plus CHX (4 ± 1%) exhibited the same level of chromatin condensation as that of mock plus CHX cells (4 ± 2%). The levels of chromatin condensation observed in vBSΔ27-infected HEp-2/HeLa in the presence (63 ± 12%) and absence (72± 5%) of CHX were comparable. However, addition of CHX during vBSΔ27 infection reduced the percentage of nuclei containing condensed chromatin in vBSΔ27-infected Vero cells from 55 ± 12% to 8 ± 4%. This difference between vBSΔ27-infected Vero cells in the presence and absence of CHX was determined to be statistically significant ($P < 0.005$). Together, these findings indicate that the inhibition of protein synthesis suppressed the development of HSV-1-dependent chromatin condensation in Vero, but not in HEp-2/HeLa cells.

Because DNA laddering was reported to occur at times greater than 24 hpi during HSV-1-dependent apoptosis of Vero cells (Galvan et al., 1999; Leopardi and Roizman, 1996; Leopardi et al., 1997), we set out in the third series to validate these findings and to test whether protein synthesis was important for this phenotype as well. HEp-2/HeLa and Vero cells were mock-infected or infected with HSV-1(KOS1.1), vBSΔ27, or CgalΔ3 in the presence and absence of CHX. At 12, 24, and 36 hpi, cells were harvested, low molecular weight DNAs were extracted, separated in an agarose gel containing ethidium bromide, and visualized by fluorescence enhancement using UV illumination as described in Materials and methods (Fig. 4).

At 12 hpi, vBSΔ27-infected HEp-2/HeLa cells displayed the highest level of obvious DNA ladders (Fig. 4, lane 3), as expected (Aubert and Blaho, 1999). At 24 hpi, only the mock- and HSV-1(KOS1.1)-infected HEp-2/HeLa cells without CHX failed to yield the presence of low molecular weight DNA (compare lanes 1 and 2 with 3–8). However, these banding patterns seemed less distinct than that of vBSΔ27-infected HEp-2/HeLa cells at 12 hpi, inasmuch as the low molecular weight DNA had migrated as smears at 24 hpi. The progression from an obvious laddering pattern at early times to a smear at late times during HSV-1-dependent apoptosis was described earlier (Aubert and

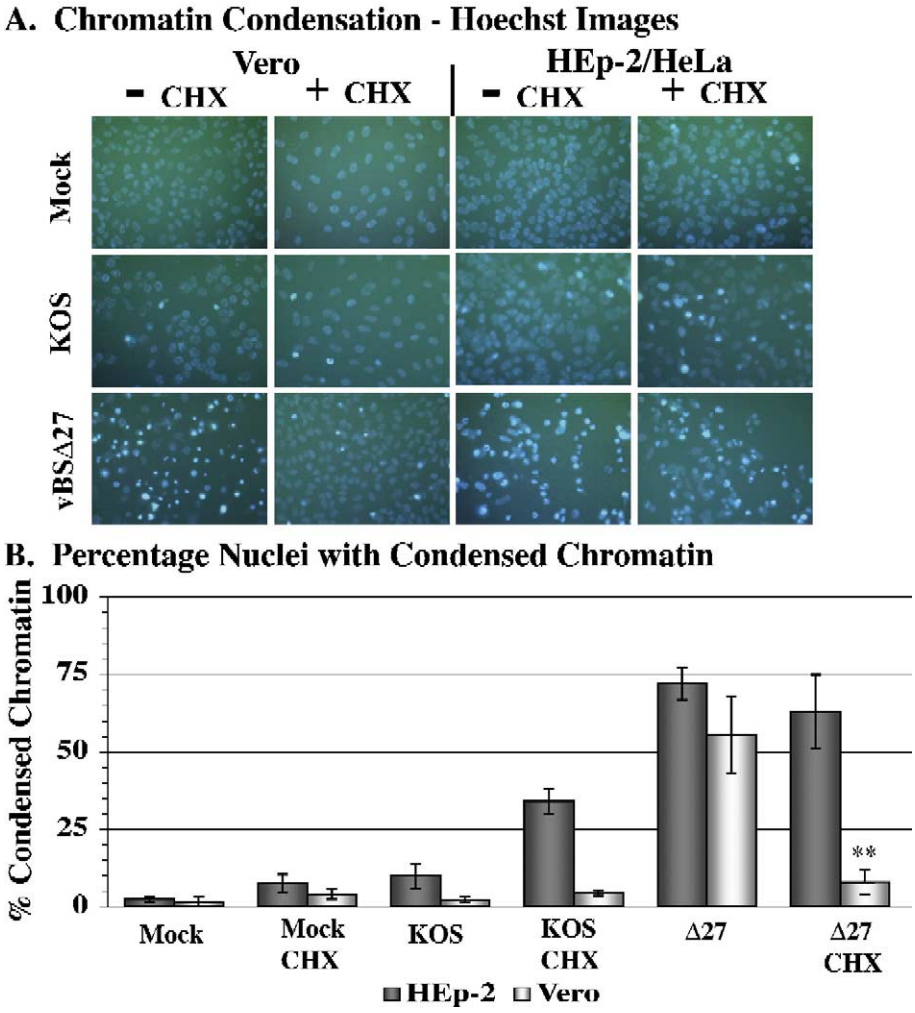

Fig. 3. Chromatin staining (A) of Vero and HEp-2/HeLa cells at 24 hpi following infection with HSV-1(KOS 1.1) and vBSΔ27 viruses in the presence (+) or absence (−) of 10 μg/ml CHX. Hoechst DNA dye was added to the media at a concentration of 5 μg/ml to allow for visualization of chromatin and cells were photographed with a digital camera following fluorescent microscopy (magnification, ×40). (B) Quantification of the percentage of nuclei with condensed chromatin. This experiment was performed in triplicate. For each replicate experiment, the number of nuclei containing condensed chromatin was counted for two to three (×40) microscopic fields; at least 400 total nuclei. The bars indicate the average percentage of nuclei containing condensed chromatin. Error bars signify the standard deviation for each treatment group. Statistical analysis of the difference between the vBSΔ27-infected Vero cells in the presence and absence of CHX was performed using Student's t test (**$P < 0.005$).

Blaho, 1999). Neither smeared nor laddered low molecular weight DNA was detected in Vero cells at 12 hpi (lanes 9–16). The mock- and HSV-1(KOS1.1)-infected Vero cells plus CHX failed to demonstrate DNA laddering at 24 and 36 hpi (lanes 9 and 10, and 13 and 14). The observation that KOS plus CHX did not show DNA laddering was consistent with the absence of apoptotic morphologies and reduced PARP cleavage in similarly-treated Vero cells (Figs. 1, 2, and 3).

Obvious DNA laddering was detected at 24 hpi in vBSΔ27- and CgalΔ3-infected Vero cells without CHX (lanes 11 and 12). The pattern of this laddering did not seem to change at 36 hpi in the absence of CHX; i.e., it did not progress to a smear without detectable laddering. Surprisingly, DNA laddering was detected with vBSΔ27- and CgalΔ3-infected Vero cells in the presence of CHX (lanes 15 and 16). It should also be noted that CHX treatment did not completely ablate PARP cleavage in vBSΔ27-infected Vero cells (Fig. 2). Together, these findings suggest that a small number of apoptotic cells may remain during infection with these deletion-mutant viruses following treatment with CHX. Importantly, the DNA laddering pattern did not change in these CHX-treated infected cells between 24 and 36 hpi (lanes 15 and 16). Also, this amount of laddering never approached the extent seen with HEp-2/HeLa cells at 24 (compare lanes 11–16 with 3–8) and 36 hpi (data not shown). This result is in agreement with our earlier findings (Figs. 1 and 2) that Vero cells exhibit slower kinetics of HSV-1-dependent apoptosis than HEp-2/HeLa cells. Even though CHX drastically reduced the level of apoptotic morphologies and decreased the extent of PARP cleavage in Vero cells infected with vBSΔ27 or CgalΔ3, it did not lead to a profound decrease in the level of DNA laddering in these

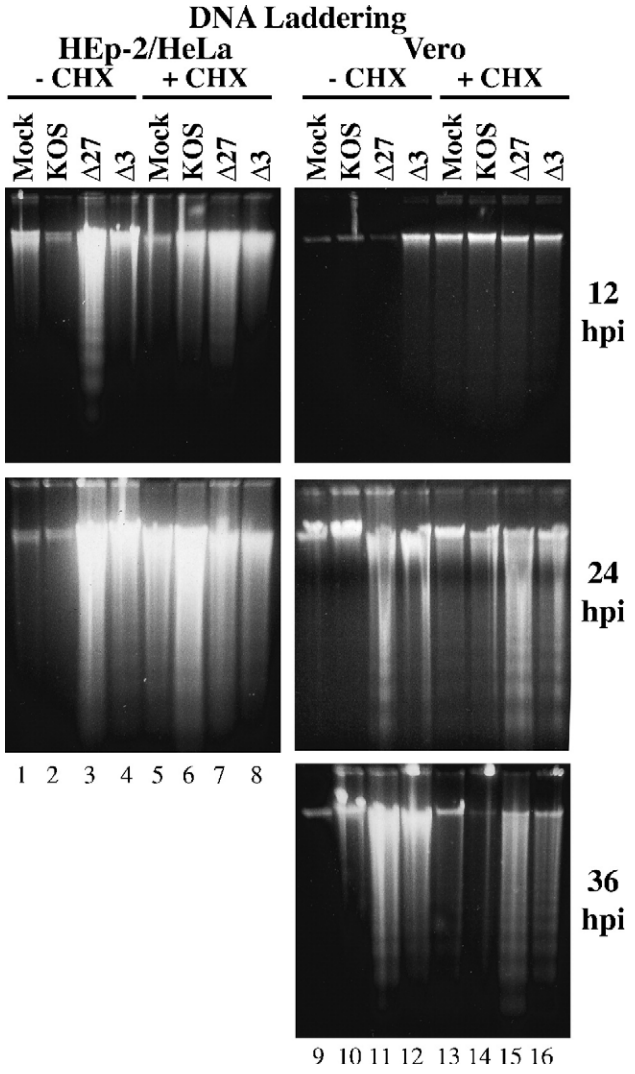

Fig. 4. Fluorescence enhancement images of nucleosomal laddering of chromosomal DNA. HEp-2/HeLa and Vero cells were infected with HSV-1(KOS 1.1), vBSΔ27 (Δ27), or CgalΔ3 (Δ3), and low molecular weight DNAs were extracted at 12, 24, and 36 hpi. Following extraction, DNAs were separated in a 2% agarose gel containing 0.1 μg/ml of ethidium bromide and visualized under UV illumination as described in Materials and methods.

cells. Thus, it appears that DNA laddering in Vero cells was not dramatically altered by CHX treatment. However, DNA laddering detection is a nonquantitative assay and the possibility remains that it may require complete prevention of apoptosis throughout the course of infection (as in mock- and KOS-infected cells) to score negatively.

Many investigators have shown that HSV-1 infection changes the composition and function of mitochondria (Galvan et al., 2000; Gautier et al., 2003; Murata et al., 2000; Radsak and Albring, 1974; Radsak and Freise, 1972; Zhou and Roizman, 2000). During apoptosis, mitochondrial membrane potential ($\Delta\psi_m$) disruption plays a key role in the induction of the intrinsic pathway and is important for amplification of the extrinsic apoptotic pathway (reviewed in Ly et al., 2003). One recent study reported that HSV-infected neuron-like cells exhibit a disruption of $\Delta\psi_m$ at 3 hpi (Gautier et al., 2003). At this time point, these researchers did not detect a similar disruption in HSV-infected Vero cells. To determine if changes in $\Delta\psi_m$ occur later during HSV-1-dependent apoptosis of Vero cells and to examine the role of protein synthesis in this process, we performed the following fourth set of experiments. HEp-2/HeLa and Vero cells were mock-infected or infected with vBSΔ27 at an MOI of 5 in the presence and absence of CHX. At 24 and 28 hpi, the cells were harvested and assessed for $\Delta\psi_m$ using the MitoCapture assay as described in Materials and methods.

MitoCapture reagent aggregates in the mitochondria of healthy cells and fluoresces red. In apoptotic cells, the MitoCapture reagent cannot penetrate mitochondria due to their disrupted mitochondrial membrane potential. Therefore, the reagent stays in its monomeric form in the cytoplasm and fluoresces green.

Using flow cytometry, we measured the red (data not shown) and green fluorescence for each cell. Representative histograms of the green (FL-1 channel) fluorescence intensity (F. I.) of Vero cells at 24 hpi are shown in Fig. 5. The single distribution observed in mock-infected cells represents F. I. of the MitoCapture Reagent (background fluorescence) in healthy cells (3%). Cells infected with vBSΔ27 displayed a bimodal F. I. distribution, indicative of a fraction of these cells undergoing apoptosis (Fig. 5C). The peak with the F. I. greater than that of background corresponds to cells with disrupted $\Delta\psi_m$. The areas under these curves were used to determine the percentage of cells with disrupted $\Delta\psi_m$ (Fig. 5 and Table 1) as described in Materials and methods.

At 24 hpi, approximately 50% of vBSΔ27-infected cells displayed disrupted $\Delta\psi_m$ in both cell lines (Fig. 5C and Table 1). CHX treatment of mock-infected HEp-2/HeLa or Vero cells at 24 hpi did not significantly alter the percentage displaying disrupted $\Delta\psi_m$ compared to mock without CHX cells (Fig. 5 and Table 1). The addition of CHX during vBSΔ27 infection led to a decrease in the percentage of Vero cells exhibiting $\Delta\psi_m$ disruption from 46% to 20% (compare Figs. 5C with D). In contrast, CHX treatment of the vBSΔ27-infected HEp-2/HeLa cells did not lead to a reduced $\Delta\psi_m$ disruption (51% and 57%) (Table 1). Similar results were observed when $\Delta\psi_m$ was measured at 28 hpi (Table 1). Thus, inhibition of protein synthesis led to a reduced disruption of $\Delta\psi_m$ in vBSΔ27-infected Vero cells, but not HEp-2/HeLa cells. This indicates that protein synthesis is required for vBSΔ27 to optimally disrupt the $\Delta\psi_m$ of Vero cells.

Taken together, the results from Figs. 1–5 and Table 1 illustrate several aspects of HSV-1-dependent apoptosis in Vero cells. First, apoptosis was induced in infected Vero cells, but we observe it at a much lower extent than that of HEp-2/HeLa cells. This observation of apoptosis in infected Vero cells is consistent with the results of others (Galvan and Roizman, 1998). Second, a significant kinetic distinc-

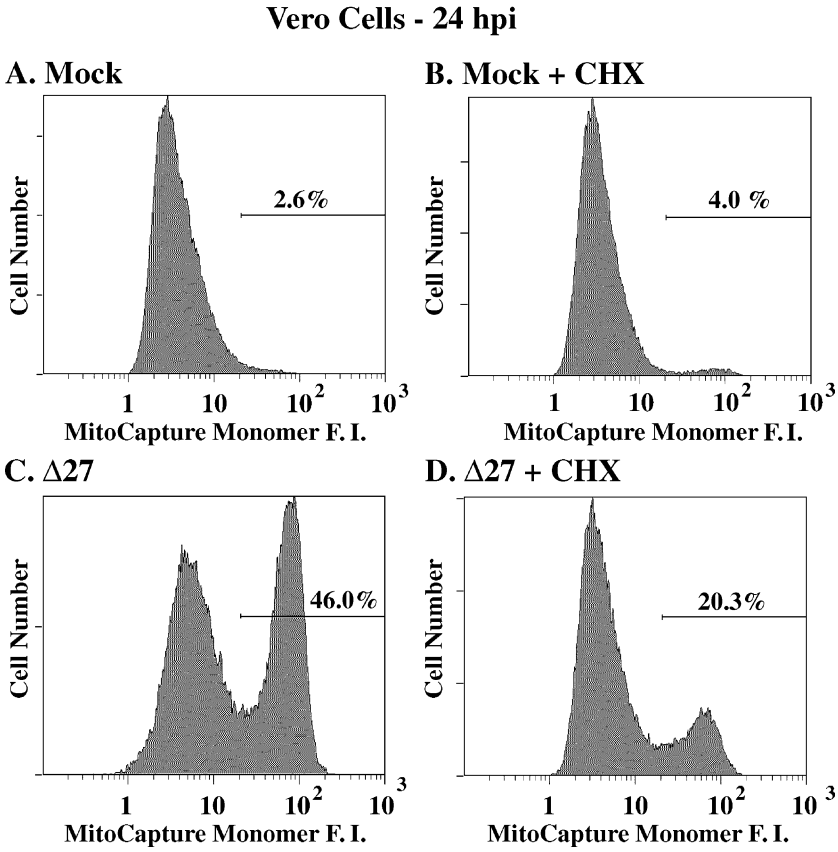

Fig. 5. Flow cytometry analysis of MitoCapture assay. Vero cells were mock (A–B)-infected or infected with vBSΔ27 (C–D) in the presence (B and D) or absence (A and C) of 10 μg/ml CHX. At 24 hpi, adherent and floating cells were harvested and assessed for mitochondrial membrane potential ($\Delta\psi_m$) using the MitoCapture assay as described in Materials and methods. In apoptotic cells, MitoCapture monomers were detected in the FL1 channel of a flow cytometer. Graphic representations of MitoCapture monomer fluorescence intensity (F. I.) are displayed. The area under the curve that displays a peak monomer F. I. greater than that of mock was used to define the percentage of cells with disrupted $\Delta\psi_m$ (numbers beside each graph). The results shown in this figure are representative of the data used to generate Table 1.

tion exists between the apoptotic responses of Vero and HEp-2/HeLa cells to HSV-1 infection. Finally, Vero cells, but not HEp-2/HeLa cells, require de novo protein synthesis to undergo efficient HSV-1-dependent apoptosis.

Table 1
Inhibition of protein synthesis reduces HSV-dependent disruption of mitochondrial membrane potential

	Percentage of cells with disrupted mitochondrial membrane potential ($\Delta\psi_m$)		
	24 hpi	28 hpi	28 hpi
Vero			
Mock	2.6	7.5	11.7
Mock + CHX	4.0	3.7	6.7
Δ27	46.0	35.0	42.8
Δ27 + CHX	20.3	18.4	27.4
HEp-2/HeLa			
Mock	6.8		25.1
Mock + CHX	7.0		17.9
Δ27	50.6		64.0
Δ27 + CHX	57.2		71.9

Protein synthesis prior to 3 hpi was required for efficient HSV-1-dependent apoptosis in Vero cells

We next set out to define the time period during HSV-1 infection that de novo protein synthesis was required for optimal apoptosis to occur in Vero cells. To accomplish this, Vero cells were infected with vBSΔ27 in intervals such that the infections were allowed to progress for 0, 1, 2, 3, and 5 h before de novo protein synthesis was blocked by the addition of CHX (Fig. 6A). Our prediction was that if CHX is added after the proteins required for HSV-1-dependent apoptosis had been synthesized, then CHX addition would not affect the level of apoptosis observed with vBSΔ27 infection in Vero cells. Concurrent infections were performed without the addition of CHX, as controls. At 24 h following CHX treatment, Hoechst dye was added to the media and microscopic images were captured to assess chromatin condensation (Fig. 6B). Subsequently, the cells were harvested, proteins were extracted, and immunoblotting analyses were performed using anti-PARP antibody (Fig. 6C).

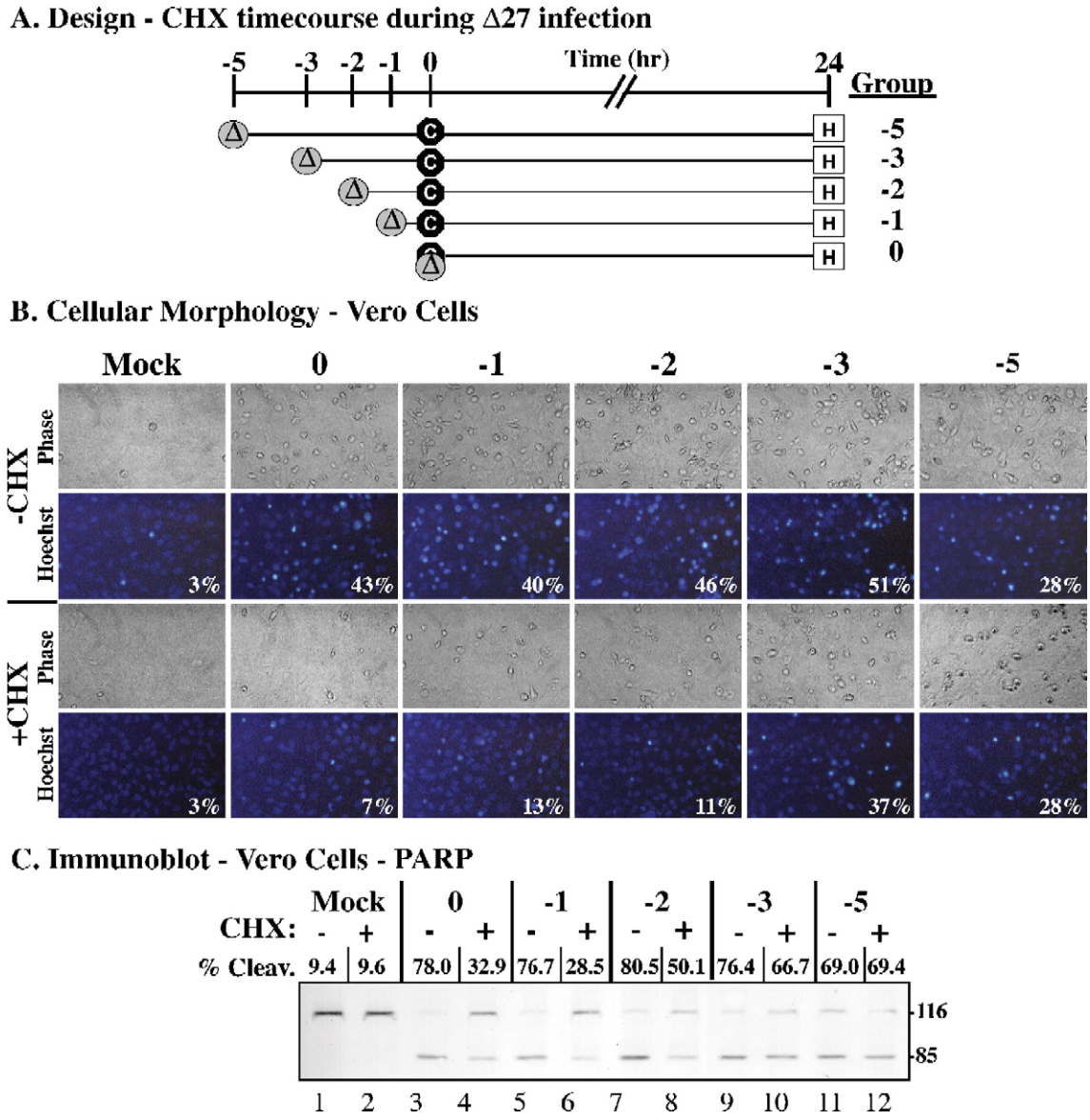

Fig. 6. Schematic representation (A), chromatin staining (B), and PARP cleavage (C) identifying the time frame in which proteins must be synthesized for HSV-1-dependent apoptosis. Infections were staggered such that CHX addition (stop sign containing "C") would block de novo protein synthesis in vBSΔ27-infected (circle containing "Δ") Vero cells at 0, 1, 2, 3, and 5 hpi. 24 h following the time of CHX treatment ($T = 0$), Hoechst dye was used to visualize condensed chromatin and whole cell extracts (square containing "H") were prepared. As controls, extracts were also prepared from mock- and vBSΔ27-infected Vero cells which were not treated with CHX. (B) Cells were photographed at 24 hpi with a digital camera following phase-contrast light (Phase) and fluorescent (Hoechst) microscopy (magnification, ×40). Numbers represent the percentage of nuclei in the panel field with condensed chromatin. (C) Immune reactivities of vBSΔ27-infected Vero cell electrophoretically separated extracts with (+) and without (−) CHX treatment. 50 μg of protein was used for immunoblot analysis with anti-PARP monoclonal antibody. The migration of the 116,000 molecular weight uncleaved (116) and 85,000 molecular weight cleaved product (85) is indicated. NIH image was used to quantify the percent PARP cleavage (% cleav.) as described in Materials and methods.

The inhibition of de novo protein synthesis by CHX addition at 0 and 1 hpi led to a reduction in chromatin condensation (7% and 13%, respectively) in the vBSΔ27-infected cells (Fig. 6B) compared to that without CHX (43% and 40%). Similarly, PARP cleavage in the presence of CHX at these times was also reduced (33% and 29%) compared to that without CHX (78% and 77%) (Fig. 6C, compare lanes 4 and 6 with 3 and 5). When CHX was added at 2 hpi (Fig 6C, compare lanes 7 and 8), there was a modest reduction in PARP cleavage (50%) compared to vBSΔ27-infected cells without CHX (81%), as well as a reduction in chromatin condensation from 46% to 11% (Fig. 6B). At 3 and 5 hpi, there was little to no reduction in PARP cleavage (67% and 69%, respectively) or chromatin condensation (37% and 28%) in the CHX-treated cells (Figs. 6B and C, lanes 11–12) compared to the controls (76% and 69% for PARP; 51% and 28% for chromatin condensation). We have also performed a similar experiment in which the harvest time was staggered and the infection time kept constant for all

treatment groups, and this analysis yielded similar results (data not shown). Based on these results, we conclude that the initiation of synthesis of protein(s) required for efficient HSV-1-dependent apoptosis in Vero cells occurs prior to 3 hpi and these factors are completely active by 5 hpi.

Synthesis of full-length ICP22 and U_S1.5 were not required for efficient HSV-1-dependent apoptosis in Vero cells

The finding that the proteins necessary for efficient HSV-1-dependent apoptosis in Vero cells are synthesized by 3 hpi suggests that either cellular proteins or IE viral proteins might play a role in the process. Our results showing reductions in PARP cleavage upon CHX treatment with vBSΔ27 or CgalΔ3 viruses indicate that the ICP27 and ICP4 IE proteins are not required for HSV-1-dependent apoptosis in Vero cells. Recent studies have shown that U_S1.5, a truncated, carboxyl-terminal version of ICP22 that begins at amino acid 147 (Carter and Roizman, 1996), can activate caspase 3 if it is highly expressed using a baculovirus vector (Hagglund et al., 2002). To determine whether U_S1.5 or ICP22 is required for HSV-1-dependent apoptosis in Vero cells, we utilized the HSV-1(DMP) virus which does not synthesize full-length ICP27 or ICP22 (Wu et al., 1996). In HSV-1(DMP), the open reading frame encoding ICP27 is deleted (McCarthy et al., 1989) and a termination codon is inserted at amino acid 199 of the 420 amino acid-long ICP22, thus producing truncated forms of ICP22 (Rice et al., 1995) and U_S1.5. A virus containing the n199 ICP22 mutant allele (Post and Roizman, 1981) exhibited a growth deficiency similar to that seen with a complete ICP22 knockout (Poffenberger et al., 1993), indicating that if any truncated proteins are produced, they are likely to be inactive. Vero cells were mock-, HSV-1(KOS1.1)-, vBSΔ27-, or HSV-1(DMP)-infected at an MOI of 5 in the presence and absence of CHX. At 24 hpi, nuclear and cellular morphologies (Fig. 7A) and the extents of PARP cleavage (Fig. 7B) were determined. To monitor viral infection, we also immunoblotted for ICP4, ICP27, and TK viral proteins.

As expected, KOS-infected cells displayed abundant levels of ICP4, ICP27, and TK, and CHX greatly reduced the levels of these proteins (compare lanes 3 and 4). ICP4 and TK, but not ICP27, were evident in vBSΔ27- and DMP-infected cells (lanes 5 and 7). Surprisingly, the levels of ICP4 and TK proteins were higher in Vero cells infected with DMP than those infected with the vBSΔ27 virus. The basis for this difference is unknown at this time.

In this experiment, the presence of CHX during vBSΔ27 infection decreased the level of chromatin condensation from 37% to 5% (Fig. 7A). Similarly, CHX treatment led to a reduction in PARP cleavage (from 44% to 8%) in vBSΔ27-infected cells (Fig. 7B, compare lane 6 with 5). Sixty-five percent of the cells infected with HSV-1(DMP) in the absence of CHX showed chromatin condensation (Fig. 7A) and the percentage of PARP cleavage exhibited by this group was 60% (Fig. 7B, lane 7). These findings, alone, suggest that the proteins required for HSV-1-dependent apoptosis in Vero cells are produced during HSV-1(DMP) infection. Furthermore, CHX addition to HSV-1(DMP)-infected cells led to a dramatic reduction in chromatin condensation (from 65% to 5%) and PARP cleavage (from 60% to 9%) (Fig. 7, compare lanes 7 and 8). Based on these results, we conclude that full-length ICP22 and U_S1.5 are not required for HSV-1-dependent apoptosis in Vero cells.

Discussion

Initial characterizations of HSV-1-dependent apoptosis mainly utilized the HEp-2/HeLa cell line. Since that time, several cell type-dependent differences in this apoptotic response have been reported. Here, we examined the differences between HSV-1-dependent apoptosis in HEp-2/HeLa and Vero cells. The significant features of our findings may be summarized as follows.

Vero cells undergo HSV-1-dependent apoptosis with delayed kinetics compared to HEp-2/HeLa cells

The finding that Vero cells in fact do undergo apoptosis, albeit later than HEp-2/HeLa cells, is consistent with reports showing that Vero cells display nucleosomal DNA cleavage at 24 and 30 hpi when infected with the ICP4-, U_S3-null virus, *d120* (Galvan et al., 1999; Leopardi and Roizman, 1996; Leopardi et al., 1997). One explanation for the delayed response of Vero cells to HSV-1-dependent apoptosis could be that the virus grows more slowly in Vero cells. However, Vero cells accumulate viral proteins at a slightly higher rate than HEp-2/HeLa cells during wild-type HSV-1 infections (Fig. 2 and Aubert and Blaho, 1999; O'Toole et al., 2003). Furthermore, wild-type HSV-1 has been reported to grow to between 2 and 5 times higher titers in Vero cells as compared to HEp-2/HeLa cells during the same time period, suggesting that the virus grows quicker in Vero cells (Petrovskis et al., 1988; Visalli and Brandt, 1991). Therefore, the distinction in the kinetics of apoptosis is unlikely to be due to a general viral replication-cycle effect.

Although the difference in apoptotic kinetics between Vero and HEp-2/HeLa cells seems subtle, it may be biologically significant (Blaho, 2004). Two major mechanisms are used by viruses to circumvent the apoptotic responses of host cells (reviewed in Koyama et al., 2003). Some viruses, such as influenza and vesicular stomatitis viruses, replicate quickly and complete their progeny virion production before the onset of apoptotic cell death (Koyama, 1995; Kurokawa et al., 1999). Other viruses, such as adenoviruses and poxviruses, encode viral proteins

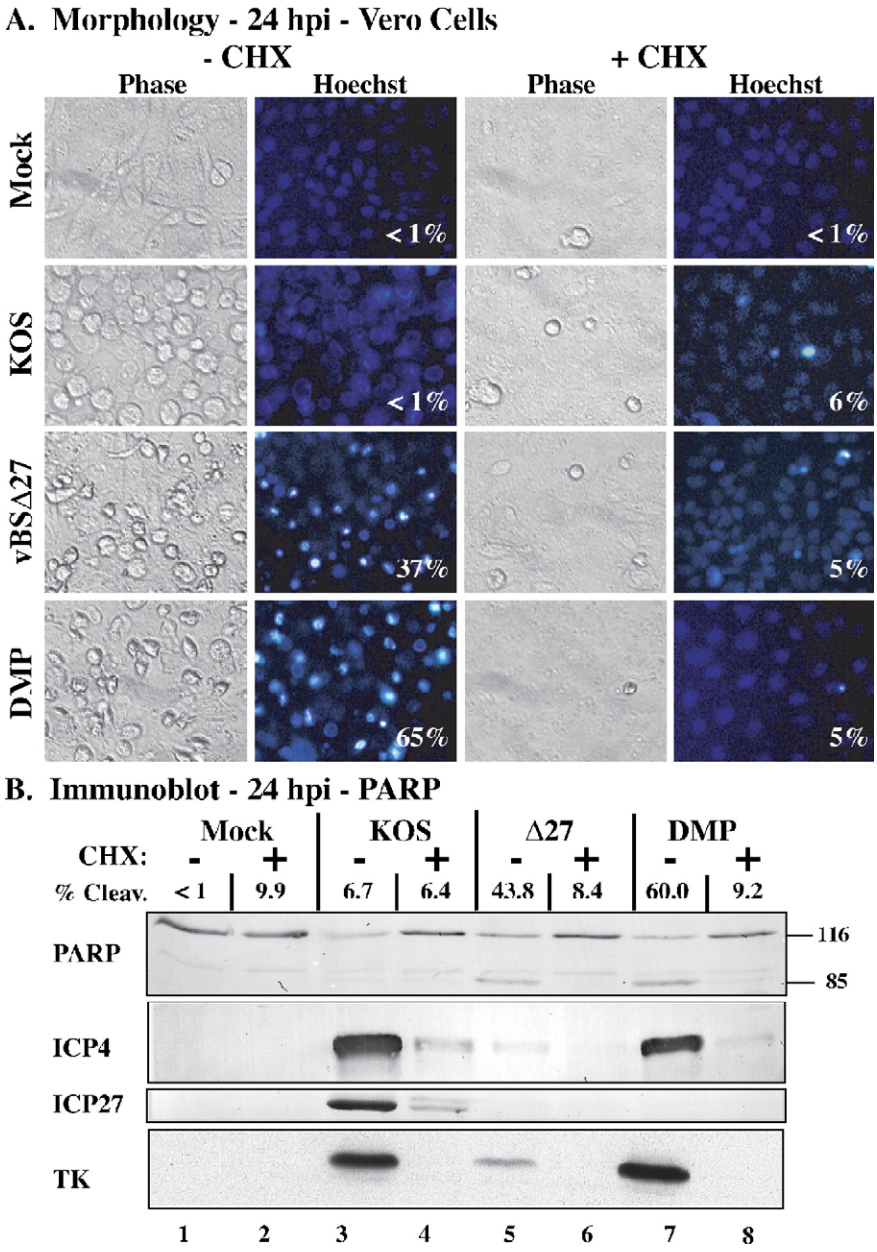

Fig. 7. Cellular morphologies (A) and immune reactivities (B) of HSV-1(DMP)-infected Vero cells. (A) Vero cells were infected with HSV-1(KOS 1.1), vBSΔ27(Δ27), or HSV-1(DMP) in the presence (+) or absence (−) of 10 μg/ml CHX. Hoechst DNA dye was added to the media at a concentration of 5 μg/ml to allow visualization of chromatin. Cells were photographed at 24 hpi with a digital camera following phase-contrast light (Phase) and fluorescent (Hoechst) microscopy (magnification, ×40). Numbers represent the percentage of nuclei in the panel field with condensed chromatin. (B) The cells in panel A were extracted and 50 μg total protein was separated in a denaturing gel and analyzed by immunoblotting using anti-PARP, anti-ICP4, and anti-thymidine kinase (TK) antibodies. The migration of the 116,000 molecular weight uncleaved (116) and 85,000 molecular weight cleaved (85) PARP products is indicated. Percent PARP cleavage (% cleav.) was calculated as described in Materials and methods.

which inhibit the apoptotic pathways (reviewed in Everett and McFadden, 2002; White, 2001). In Vero cells, the HSV-1 life cycle takes about 18 h to complete. We have shown here that apoptosis is not detected in Vero cells until 24 hpi. This result, along with the fact that HSV-1 encodes antiapoptotic proteins, suggests that in Vero cells, HSV-1 may use both of the strategies described above, i.e., rapid multiplication and antiapoptotic gene production, to evade host cell apoptosis.

Vero cells require de novo protein synthesis to undergo efficient HSV-1-dependent apoptosis while HEp-2/HeLa cells do not

This represents another significant distinction between the HSV-1-dependent apoptosis of Vero and HEp-2/HeLa cells; evidenced by the very low level of apoptosis in KOS plus CHX-treated Vero cells and the reduction in vBSΔ27- and CgalΔ3-induced apoptosis in Vero cells with CHX

treatment. It is of interest to note that we could not detect a decrease in DNA laddering in vBSΔ27- or CgalΔ3-infected Vero cells when treated with CHX even though apoptotic morphologies, mitochondrial membrane potential disruption, and PARP cleavage were reduced. Instead, the extent and patterning of laddering were unchanged from 24 to 36 hpi under these conditions. One explanation for this might be that DNA laddering is a sensitive but non-quantitative assay, in which low levels of apoptotic cells are readily detected. Also, the presence of CHX led to a great reduction, but not complete inhibition of apoptotic morphologies, mitochondrial membrane disruption, and PARP cleavage in vBSΔ27- or CgalΔ3-infected cells. Perhaps the low numbers of Vero cells that are undergoing apoptosis under these conditions are enough to make the population score positively in the DNA laddering assay. This is supported by the observation that mock-infected HEp-2/HeLa in the presence of CHX cells displayed a modest level of nucleosomal laddering at 24 hpi even though less that 10% of the cells displayed other apoptotic phenotypes at this time point. Alternatively, it may be possible in these cells to prevent caspase activities and apoptotic morphological changes without inhibiting nucleosomal DNA cleavage.

Proteins synthesized prior to 3 hpi are required for efficient apoptosis in infected Vero cells

This suggests that the synthesis of either cellular or viral protein(s) is necessary for HSV-1-dependent apoptosis in Vero cells, and our results indicate that ICP27, ICP4, full-length ICP22, and $U_S1.5$ are not required. These findings are perhaps not surprising since earlier studies have shown that ICP4 (Aubert and Blaho, 2003; Leopardi and Roizman, 1996), ICP27 (Aubert and Blaho, 1999), and ICP22 (Aubert et al., 1999) are needed for efficient apoptosis prevention. It should be noted that the data showing an antiapoptotic role for ICP22 utilized a recombinant virus containing a deletion mutation that also disrupted the $U_S1.5$ open reading frame. As the ICP4-null *d*120 virus also contains a deletion of the U_S3 gene (Leopardi et al., 1997) and this virus triggers apoptosis in Vero cells (Leopardi and Roizman, 1996), we must conclude that U_S3 is also not required for HSV-1-dependent apoptosis in these cells. Since U_S3 is a late gene (Roizman and Knipe, 2001), this conclusion is consistent with our finding that the required protein(s) is produced prior to 3 hpi. This leaves open the possibility that synthesis of ICP0 and/or ICP47 viral proteins may participate in HSV-1-dependent apoptosis in Vero cells. However, it should be noted that data have recently been published which imply an antiapoptotic function for the ICP0 protein, due to its ability to ubiquitinate p53 and target it for degradation (Boutell and Everett, 2003).

Alternatively, cellular protein synthesis may be required for HSV-1-dependent apoptosis in Vero cells. If this is the case, the required cellular proteins most likely induce apoptosis as an antiviral response. At least two previous studies from our laboratory are consistent with a host antiviral role for apoptosis; in each, apoptosis prevention during HSV-1 infection increases the accumulation of viral gene products. First, the addition of the caspase 3 inhibitor, Z-DEVD-fmk, to vBSΔ27-infected HEp-2/HeLa cells increases the steady state level of IE ICP4 protein (Aubert et al., 1999). Second, inducing antiapoptotic pathways by addition of the phorbol ester PMA in vBSΔ27-infected HEp-2/HeLa cells increases the level of ICP4 accumulation (Goodkin et al., 2003). Still, the cellular mechanisms that mediate antiviral apoptosis induction remain unclear. Interestingly, infection of HeLa or baby hamster kidney cells with replication-defective mutants of HSV-1 was reported to reduce levels of antiapoptotic bcl-2 in a p38MAPK-dependent manner (Zachos et al., 2001). This result might provide examples of cellular proteins that may participate in the induction of apoptosis during HSV-1 infection.

Potential host factors that mediate the requirement for protein synthesis during HSV-1-dependent apoptosis

Our results indicate that Vero cells require protein synthesis for efficient HSV-1-dependent apoptosis while HEp-2/HeLa cells do not. HEp-2/HeLa and Vero cells possess a number of different properties that could account for this distinction. HEp-2 cells were initially reported to be derived from a human laryngeal carcinoma (Moore et al., 1955) and subsequent studies have demonstrated that those obtained from the ATCC represent a HeLa cell contamination (Chen, 1988; Nelson-Rees et al., 1974; Ogura et al., 1993). Regardless, HEp-2/HeLa cells remain a transformed, human, epithelial cell line. In contrast, Vero cells were generated through the sequential passage of adult African green monkey kidney cells (Rhim et al., 1969), and they are a nontransformed, primate, fibroblast cell line. This raises the possibility that differences in species, tissue origin, or oncogenic transformation status may be responsible for the distinct responses of Vero and HEp-2/HeLa cells to HSV-1-dependent apoptosis. However, recent preliminary experiments in our laboratory demonstrate that a nontransformed human epithelial cell line also requires protein synthesis for HSV-1-dependent apoptosis (unpublished data). This suggests that the requirement for protein synthesis during HSV-1-dependent apoptosis is not specific to primate or fibroblast cells. We are currently examining the role of oncogenic transformation status in defining the requirement for protein synthesis during HSV-1-dependent apoptosis.

Alternatively, the distinction between the apoptotic responses of HEp-2/HeLa and Vero cells may be more specific to HSV infection. HSV has recently been shown to enter Vero and HeLa cells through different pathways (Nicola et al., 2003; Nicola and Straus, 2004). HSV may enter HeLa and Chinese hamster ovary cells through an endocytic mechanism, while it enters Vero cells through

direct penetration of the cell surface. Presumably, HSV also enters HEp-2/HeLa cells through an endocytic mechanism. Regardless, we have previously shown that like HEp-2/HeLa cells, S3 HeLa cells are capable of undergoing HSV-dependent apoptosis in the absence of de novo protein synthesis (Aubert and Blaho, 2003). Therefore, it is possible that the different requirements for protein synthesis during HSV-dependent apoptosis are mediated by different entry mechanisms. Yet, it is not known at this time how endocytosis entry of HSV would substitute for the requirement for protein synthesis during HSV-dependent apoptosis.

In summary, the data included in this report provide an explanation for the different apoptotic responses of HEp-2/HeLa and Vero cells to HSV-1 infection. Differences in HSV-1-dependent apoptosis have been reported for a number of cell types including human corneal epithelial (Miles et al., 2003), mouse embryo fibroblast (Aubert and Blaho, 2003), and human neuroblastoma (Galvan and Roizman, 1998) cells. Similar temporal delays and differential requirements for protein synthesis might explain the differences observed in the HSV-1-dependent apoptosis of these and other cell types. Consideration of our findings would be beneficial to those characterizing virus–host interactions as they emphasize the impact of cell type differences in experimental systems.

Materials and methods

Cells and viruses

HEp-2/HeLa and Vero cells were obtained from the American Type Culture Collection (Rockville, MD) and maintained in Dulbecco's modified Eagle's medium (DMEM) supplemented with 5% fetal bovine serum. Although HEp-2 cells were originally developed from a patient with laryngeal carcinoma (Moore et al., 1955), it was later recognized that current isolates provided by the ATCC are HeLa cell contaminants (Chen, 1988; Nelson-Rees et al., 1974). For this reason, we refer to them as HEp-2/HeLa cells. Vero 2.2 (Heeg et al., 1986) and FO6 (Samaniego et al., 1997) cells are derivatives of Vero cells expressing either ICP27 alone or ICP27, ICP4, and ICP0 from their own promoters, respectively. HSV-1(KOS1.1) was the strain of wild-type HSV-1 used in this study. HSV-1(CgalΔ3) and HSV-1(vBSΔ27) viruses were generously provided by Theodore Friedmann and Saul Silverstein, respectively. vBSΔ27 is an ICP27-null virus derived from HSV-1(KOS 1.1) containing a replacement of the α27 gene with the *Escherichia coli* lacZ gene (Soliman et al., 1997). This virus was propagated and tittered on Vero 2.2 (gift of Saul Silverstein). CgalΔ3 was derived from the HSV-1(17syn$^+$) strain and is an IE3 (ICP4)-null virus which is deleted for 3.6 kb of the coding region of IE3 (Paterson et al., 1990) due to having the *Escherichia coli* lacZ gene inserted into the *Bam*HI Z fragment (Johnson et al., 1992). The HSV-1(DMP) virus was generously provided by Neal DeLuca and is derived from HSV-1(KOS1.1) (Wu et al., 1996). In HSV-1(DMP), the open reading frame encoding ICP27 is deleted (McCarthy et al., 1989) and a termination codon was inserted at amino acid 199 of the 420 amino acid long ICP22 (Rice et al., 1995). CgalΔ3 and DMP viruses were propagated and tittered on FO6 cells (gift of Neal DeLuca). Cell monolayers (approximately 6×10^6) were infected at a multiplicity of infection (MOI) of 10, unless otherwise noted, and allowed to proceed at 37 °C in growth media for the times indicated in the text. In experiments designed to inhibit protein synthesis, cycloheximide (CHX) was added directly to the media at a concentration of 10 μg/ml 1 h prior to infection (excluding the time course) and maintained at that level until the time of harvest. Unless otherwise noted, all cell culture reagents were obtained from Life Technologies and all biochemicals from Sigma.

Whole cell protein extractions and immunoblotting

Whole cell extractions of infected cells were performed as follows. Cells were scraped into the medium, collected by centrifugation for 5 min at 1000 × *g*, and washed once in cold phosphate-buffered saline (PBS). Cells were lysed by resuspending in RIPA buffer (50 mM Tris–HCl, pH 7.5, 150 mM NaCl, 1% Triton X100, 1% deoxycholate, 0.1% SDS) supplemented with 2 mM phenylmethylsulfonyl fluoride (PMSF, freshly prepared stock), 1% Translysol, 0.1 mM L-I-chloro-3-(4-tosulamido)-4-phenyl-2-butanone (TPCK), 0.01 mM L-1-chlor-3-(4-tosylanmido)-7-amino-2-heptanon-hydrochloride (TLCK), and vortexed for 30 s. The cell lysates were cleared by centrifuging for 10 min at 4 °C at 16,000 × *g*. Protein concentrations were determined using a modified Bradford protein assay (Bio-Rad Laboratories). 50 μg of total protein was separated on 15% *N,N′*-diallyltartardiamide-acrylamide gels and electrically transferred to nitrocellulose using a tank apparatus (Bio-Rad Laboratories). Membranes were blocked for 1 h at room temperature in PBS containing 5% nonfat dry milk and incubated overnight at 4 °C in primary antibody. The monoclonal anti-ICP4, 1114, (Goodwin Institute for Cancer Research, Plantation, FL.), monoclonal anti-ICP27, 1113, (Goodwin), monoclonal anti-PARP (Pharmingin), and polyclonal anti-thymidine kinase (TK) antibodies were diluted at a concentration of 1:1000 in Tris-buffered saline containing 0.1% Tween 20 (TBST) and 0.1% BSA. After washing in TBST, membranes were incubated with either anti-mouse or anti-rabbit antibodies conjugated to alkaline phosphatase (Southern Biotech) diluted in blocking buffer (1:1000) for 1 h at room temperature. Following washing in TBST, immunoblots were developed in buffer containing 5-bromo-4-chloro-3-indolyl phosphate and 4-nitro-bluetetrazolium chloride.

Densitometric analysis

To quantitate the percentage of total infected cell PARP that is cleaved, densitometry of immune reactive PARP was performed as described (Aubert et al., 1999). NIH image version 1.63 was used to measure the integrated density (ID) of the 116,000 molecular weight uncleaved and 85,000 molecular weight cleaved PARP bands. These values were used to calculated the % PARP cleavage (cleav.) for each lane using the following formula: % cleav. = {(cleaved PARP ID)/(cleaved PARP ID plus uncleaved PARP ID)} × 100%.

DNA laddering assay

Nucleosomal cleavage of cellular DNA was assessed essentially as described previously (Aubert and Blaho, 1999; Koyama and Miwa, 1997). Briefly, cells were scraped into the medium, collected by centrifugation for 5 min at 1000 × *g*, and washed once in cold PBS. Following suspension in 100 μl of PBS, the cells were lysed by the addition of 400 μl of 10 mM Tris–HCl, pH 7.4, 10 mM EDTA containing 0.6% SDS. Lysates were mixed with 125 μl of 5 M NaCl and after overnight incubation at 4 °C, the solution was centrifuged for 30 min at 16,000 × *g* to pellet chromosomal DNA. The supernatant was then subjected to treatment with 0.1 mg/ml RNAse A (37 °C for 1 h) and 1 mg/ml Proteinase K (50 °C for 2 h), followed by sequential phenol/chloroform extractions and precipitation in ethanol. The precipitated DNA was resuspended in water. Subsequently, the entire sample volume was separated in a 2% agarose gel using 89 mM Tris-borate, pH 8.3, 2 mM EDTA running buffer containing 0.1 μg/ml ethidium bromide and visualized using UV illumination.

Microscopic analysis, image capture, and quantification of chromatin condensation

The morphologies of infected cells were visualized by phase contrast and fluorescence light microscopy and documented using an Olympus IX70/IX-FLA inverted fluorescence microscope. Images were acquired with a Sony DKC-5000 digital camera linked to a PowerMac workstation and processed through Adobe Photoshop. For chromatin condensation analysis, 5 μg/ml Hoechst 33258 (Sigma) was added to the media. Quantification of chromatin condensation was determined by counting the number of brightly stained, small nuclei in several microscopic fields. The percentage of nuclei containing condensed chromatin was determined using two independent methods. (i) As an initial gauge of apoptosis, infected cells, which were to be extracted for later immunoblotting studies, were analyzed. The nuclei of these cells containing condensed chromatin were counted in a particular (40×) microscopic field. These numbers are presented as percentages displayed within panels in figures showing Hoechst-stained nuclei. It should be noted that fields counted are slightly larger than the displayed images. At least 100 total nuclei were counted per treatment group. (ii) To specifically determine the significance of changes in chromatin condensation observed upon CHX addition, detailed counting experiments were performed in triplicate. The percentage of nuclei with condensed chromatin was assessed in two to three (40×) fields per replicate. This resulted in the counting of over 400 nuclei per treatment group. Values from the three experiments were averaged, standard deviations calculated, and statistical analysis was then performed using the two-sided Student's *t* test.

MitoCapture assay

Following infection and/or CHX treatment, cell culture media were removed and reserved. Adherent cells were removed from culture vessels by rinsing once in PBS, then incubating in a 0.5 mg/ml Trypsin, 0.53 mM EDTA solution, and dislodged by repeat-pipetting. The trypsinized cells were then combined with the media which had been removed from the culture vessel. Cells from media and monolayers were then collected by centrifuging for 5 min at 500 × *g* and washed once with PBS. Next, cells with disrupted mitochondrial membrane potential were identified using the MitoCapture Kit (BioVision), as per the manufacturer's instructions. Briefly, approximately 6×10^6 of harvested/washed cells were suspended in 1 ml of diluted MitoCapture reagent and incubated at 37 °C for 20 min. The labeled cells were centrifuged at 500 × *g* for 5 min. The pellet was suspended in 1 ml of prewarmed MitoCapture buffer. In healthy, nonapoptotic cells, the MitoCapture reagent aggregates in mitochondria and fluoresces in the red spectra. When the mitochondrial membrane potential is disrupted in apoptotic cells, the MitoCapture reagent remains in the cytoplasm as monomers. These monomers fluoresce in the green spectra. MitoCapture-labeled cells were analyzed for green (in the FL1 channel) and red (in the FL2 channel) fluorescence using a Beckman Coulter Cytomics FC500 flow cytometer. The percentage of cells with disrupted mitochondrial membrane potential was determined using Cytometics RXR flow cytometry software and these fluorescence intensities (both FL1 and FL2) were plotted. In control studies, staurosporine-treated, apoptotic HEp-2 and Vero cells labeled with MitoCapture reagent displayed an increase in FL1 fluorescence intensity and a decrease in FL2 fluorescence intensity compared to untreated controls (data not shown). Since the change in signal intensity is greater in the FL1 (green) channel due to the intrinsic nature of the MitoCapture reagent, the non-apoptotic and apoptotic populations are more readily discerned using this channel. Thus, we focused our analysis on the FL1 channel. Accordingly, cells with reduced FL1 fluorescence were defined as cells with disrupted mitochondrial membrane potential. The low level FL1 fluorescence intensity peak observed in mock-treated cells corresponds to

background fluorescence of the MitoCapture Reagent when it is inside healthy cells. The distribution of cells with peak FL1 fluorescence intensity greater than that of this background fluorescence was defined as the distribution of cells with disrupted mitochondrial membrane potential (disrupted $\Delta\psi_m$ curve). This curve was used to calculate the percentage of cells with disrupted $\Delta\psi_m$ using the following equation: % cells with disrupted $\Delta\psi_m$ = area under the disrupted $\Delta\psi_m$ curve/(area under disrupted $\Delta\psi_m$ curve + area under background curve) × 100%.

During the course of this study, we have attempted to set up Annexin V staining and low molecular weight monitoring procedures with FACS analysis in our laboratory. However, as of yet, we have not been able to optimize the assays to our satisfaction. We believe this is mainly due to the inherent complications with using adherent cells (such as Veros and Hep-2/HeLa cells) in flow cytometry analysis.

Acknowledgments

We thank Elise Morton (MSSM) for expert technical cell culture assistance and Neal DeLuca (Univ. of Pittsburgh) for generously providing the HSV-1(DMP) virus. We are grateful to Jamie Yedowitz (MSSM) for her invaluable assistance in optimizing the MitoCapture assay and thank Ana Fernandez-Sesma (MSSM) for her expert advice in flow cytometry analysis. These studies were supported in part by a grant from the USPHS (AI48582 to J.A.B.). M.L.N. is a postdoctoral trainee and was supported in part by USPHS Institutional Research Training Awards (AI07647 and CA088796). R.M.K. was supported in part by an Undergraduate Research Fellowship from the Howard Hughes Medical Institute to Manhattan College, Riverdale, NY.

References

Aubert, M., Blaho, J.A., 1999. The herpes simplex virus type 1 regulatory protein ICP27 is required for the prevention of apoptosis in infected human cells. J. Virol. 73 (4), 2803–2813.

Aubert, M., Blaho, J.A., 2001. Modulation of apoptosis during HSV infection in human cells. Microbes Infect. 3, 859–866.

Aubert, M., Blaho, J.A., 2003. Viral oncoapoptosis of human tumor cells. Gene Ther. 10 (17), 1437–1445.

Aubert, M., O'Toole, J., Blaho, J.A., 1999. Induction and prevention of apoptosis in human HEp-2 cells by herpes simplex virus type 1. J. Virol. 73 (12), 10359–10370.

Aubert, M., Rice, S.A., Blaho, J.A., 2001. Accumulation of herpes simplex type 1 early and leaky-late proteins correlates with the prevention of apoptosis in infected human HEp-2 cells. J. Virol. 75, 1013–1030.

Avitabile, E., Di Gaeta, S., Torrisi, M.R., Ward, P.L., Roizman, B., Campadelli-Fiume, G., 1995. Redistribution of microtubules and Golgi apparatus in herpes simplex virus-infected cells and their role in viral exocytosis. J. Virol. 69 (12), 7472–7482.

Blaho, J.A., 2004. Virus infection and apoptosis (issue II) an introduction: cheating death or death as a fact of life? Int. Rev. Immunol. 23 (1–2), 1–6.

Boutell, C., Everett, R.D., 2003. The herpes simplex virus type 1 (HSV-1) regulatory protein ICP0 interacts with and ubiquitinates p53. J. Biol. Chem. 278 (38), 36596–36602.

Carter, K.L., Roizman, B., 1996. The promoter and transcriptional unit of a novel herpes simplex virus 1 alpha gene are contained in, and encode a protein in frame with, the open reading frame of the alpha 22 gene. J. Virol. 70 (1), 172–178.

Chen, T.R., 1988. Re-evaluation of HeLa, HeLa S3, and HEp-2 karyotypes. Cytogenet. Cell Genet. 48 (1), 19–24.

DeLuca, N.A., Schaffer, P.A., 1985. Activation of immediate-early, early, and late promoters by temperature-sensitive and wild-type forms of herpes simplex virus type 1 protein ICP4. Mol. Cell Biol. 5 (8), 1997–2208.

DeLuca, N.A., McCarthy, A.M., Schaffer, P.A., 1985. Isolation and characterization of deletion mutants of herpes simplex virus type 1 in the gene encoding immediate-early regulatory protein ICP4. J. Virol. 56 (2), 558–570.

Dixon, R.A., Schaffer, P.A., 1980. Fine-structure mapping and functional analysis of temperature-sensitive mutants in the gene encoding the herpes simplex virus type 1 immediate early protein VP175. J. Virol. 36 (1), 189–203.

Everett, H., McFadden, G., 2002. Poxviruses and apoptosis: a time to die. Curr. Opin. Microbiol. 5 (4), 395–402.

Galvan, V., Roizman, B., 1998. Herpes simplex virus 1 induces and blocks apoptosis at multiple steps during infection and protects cells from exogenous inducers in a cell-type-dependent manner. Proc. Natl. Acad. Sci. U.S.A. 95 (7), 3931–3936.

Galvan, V., Brandimarti, R., Roizman, B., 1999. Herpes simplex virus 1 blocks caspase-3-independent and caspase-dependent pathways to cell death. J. Virol. 73 (4), 3219–3226.

Galvan, V., Brandimarti, R., Munger, J., Roizman, B., 2000. Bcl-2 blocks a caspase-dependent pathway of apoptosis activated by herpes simplex virus 1 infection in HEp-2 cells. J. Virol. 74 (4), 1931–1938.

Gautier, I., Coppey, J., Durieux, C., 2003. Early apoptosis-related changes triggered by HSV-1 in individual neuronlike cells. Exp. Cell Res. 289 (1), 174–183.

Goodkin, M.L., Ting, A.T., Blaho, J.A., 2003. NF-kappaB is required for apoptosis prevention during herpes simplex virus type 1 infection. J. Virol. 77 (13), 7261–7280.

Goodkin, M.L., Morton, E.R., Blaho, J.A., 2004. Herpes simplex virus infection and apoptosis. Int. Rev. Immunol. 23 (1–2), 141–172.

Hagglund, R., Munger, J., Poon, A.P., Roizman, B., 2002. U (S)3 protein kinase of herpes simplex virus 1 blocks caspase 3 activation induced by the products of U (S)1.5 and U (L)13 genes and modulates expression of transduced U (S)1.5 open reading frame in a cell type-specific manner. J. Virol. 76 (2), 743–754.

Hampar, B., Elison, S.A., 1961. Chromosomal aberrations induced by an animal virus. Nature 192, 145–147.

Hardwicke, M.A., Vaughan, P.J., Sekulovich, R.E., O'Conner, R., Sandri-Goldin, R.M., 1989. The regions important for the activator and repressor functions of herpes simplex virus type 1 alpha protein ICP27 map to the C-terminal half of the molecule. J. Virol. 63 (11), 4590–4602.

Heeg, U., Dienes, H.P., Muller, S., Falke, D., 1986. Involvement of actin-containing microfilaments in HSV-induced cytopathology and the influence of inhibitors of glycosylation. Arch. Virol. 91 (3–4), 257–270.

Jerome, K.R., Fox, R., Chen, Z., Sears, A.E., Lee, H., Corey, L., 1999. Herpes simplex virus inhibits apoptosis through the action of two genes, Us5 and Us3. J. Virol. 73 (11), 8950–8957.

Johnson, P.A., Miyanohara, A., Levine, F., Cahill, T., Friedmann, T., 1992. Cytotoxicity of a replication-defective mutant of herpes simplex virus type 1. J. Virol. 66 (5), 2952–2965.

Kerr, F.R., Harmon, B.V., 1991. Definition and incidence of apoptosis: an historical perspective. In: Tomei, L.D., Cope, F.O. (Eds.), Apoptosis: the Molecular Basis of Cell Death. Cold Sprong Harbor Laboratory, Cold Spring Harbor, NY, pp. 5–29.

Kerr, J.F., Wyllie, A.H., Currie, A.R., 1972. Apoptosis: a basic biological phenomenon with wide-ranging implications in tissue kinetics. Br. J. Cancer 26 (4), 239–257.

Koyama, A.H., 1995. Induction of apoptotic DNA fragmentation by the infection of vesicular stomatitis virus. Virus Res. 37 (3), 285–290.

Koyama, A.H., Adachi, A., 1997. Induction of apoptosis by herpes simplex virus type 1. J. Gen. Virol. 78 (Pt. 11), 2909–2912.

Koyama, A.H., Miwa, Y., 1997. Suppression of apoptotic DNA fragmentation in herpes simplex virus type 1-infected cells. J. Virol. 71 (3), 2567–2571.

Koyama, A.H., Adachi, A., Irie, H., 2003. Physiological significance of apoptosis during animal virus infection. Int. Rev. Immunol. 22 (5–6), 341–359.

Kurokawa, M., Koyama, A.H., Yasuoka, S., Adachi, A., 1999. Influenza virus overcomes apoptosis by rapid multiplication. Int. J. Mol. Med. 3 (5), 527–530.

Leopardi, R., Roizman, B., 1996. The herpes simplex virus major regulatory protein ICP4 blocks apoptosis induced by the virus or by hyperthermia. Proc. Natl. Acad. Sci. U.S.A. 93 (18), 9583–9587.

Leopardi, R., Van Sant, C., Roizman, B., 1997. The herpes simplex virus 1 protein kinase US3 is required for protection from apoptosis induced by the virus. Proc. Natl. Acad. Sci. U.S.A. 94 (15), 7891–7896.

Ly, J.D., Grubb, D.R., Lawen, A., 2003. The mitochondrial membrane potential (deltapsi (m)) in apoptosis; an update. Apoptosis 8 (2), 115–128.

McCarthy, A.M., McMahan, L., Schaffer, P.A., 1989. Herpes simplex virus type 1 ICP27 deletion mutants exhibit altered patterns of transcription and are DNA deficient. J. Virol. 63 (1), 18–27.

Miles, D., Athmanathan, S., Thakur, A., Willcox, M., 2003. A novel apoptotic interaction between HSV-1 and human corneal epithelial cells. Curr. Eye Res. 26 (3–4), 165–174.

Moore, A.E., Sabachewsky, L., Toolan, H.W., 1955. Culture characteristics of four permanent lines of human cancer cells. Cancer Res. 15, 598–605.

Murata, T., Goshima, F., Daikoku, T., Inagaki-Ohara, K., Takakuwa, H., Kato, K., Nishiyama, Y., 2000. Mitochondrial distribution and function in herpes simplex virus-infected cells. J. Gen. Virol. 81 (Pt. 2), 401–406.

Nelson-Rees, W.A., Zhdanov, V.M., Hawthorne, P.K., Flandermeyer, R.R., 1974. HeLa-like marker chromosomes and type-A variant glucose-6-phosphate dehydrogenase isoenzyme in human cell cultures producing Mason–Pfizer monkey virus-like particles. J. Natl. Cancer Inst. 53 (3), 751–757.

Nicola, A.V., Straus, S.E., 2004. Cellular and viral requirements for rapid endocytic entry of herpes simplex virus. J. Virol. 78 (14), 7508–7517.

Nicola, A.V., McEvoy, A.M., Straus, S.E., 2003. Roles for endocytosis and low pH in herpes simplex virus entry into HeLa and Chinese hamster ovary cells. J. Virol. 77 (9), 5324–5332.

O'Toole, J.M., Aubert, M., Kotsakis, A., Blaho, J.A., 2003. Mutation of the protein tyrosine kinase consensus site in the herpes simplex virus 1 alpha22 gene alters ICP22 posttranslational modification. Virology 305 (1), 153–167.

Ogura, H., Yoshinouchi, M., Kudo, T., Imura, M., Fujiwara, T., Yabe, Y., 1993. Human papillomavirus type 18 DNA in so-called HEP-2, KB and FL cells-further evidence that these cells are HeLa cell derivatives. Cell. Mol. Biol. (Noisy-le-grand) 39 (5), 463–467.

Paterson, T., Preston, V.G., Everett, R.D., 1990. A mutant of herpes simplex virus type 1 immediate early polypeptide Vmw175 binds to the cap site of its own promoter in vitro but fails to autoregulate in vivo. J. Gen. Virol. 71 (Pt. 4), 851–861.

Perkins, D., Gyure, K.A., Pereira, E.F., Aurelian, L., 2003. Herpes simplex virus type 1-induced encephalitis has an apoptotic component associated with activation of c-Jun N-terminal kinase. J. NeuroVirol. 9 (1), 101–111.

Perng, G.C., Jones, C., Ciacci-Zanella, J., Stone, M., Henderson, G., Yukht, A., Slanina, S.M., Hofman, F.M., Ghiasi, H., Nesburn, A.B., Wechsler, S.L., 2000. Virus-induced neuronal apoptosis blocked by the herpes simplex virus latency-associated transcript. Science 287 (5457), 1500–1503.

Petrovskis, E.A., Meyer, A.L., Post, L.E., 1988. Reduced yield of infectious pseudorabies virus and herpes simplex virus from cell lines producing viral glycoprotein gp50. J. Virol. 62 (6), 2196–2199.

Poffenberger, K.L., Raichlen, P.E., Herman, R.C., 1993. In vitro characterization of a herpes simplex virus type 1 ICP22 deletion mutant. Virus Genes 7 (2), 171–186.

Post, L.E., Roizman, B., 1981. A generalized technique for deletion of specific genes in large genomes: alpha gene 22 of herpes simplex virus 1 is not essential for growth. Cell 25 (1), 227–232.

Preston, C.M., 1979. Control of herpes simplex virus type 1 mRNA synthesis in cells infected with wild-type virus or the temperature-sensitive mutant tsK. J. Virol. 29 (1), 275–284.

Radsak, K., Albring, M., 1974. Stimulation of mitochondrial DNA synthesis as an early function of herpes simplex virus. FEBS Lett. 44 (2), 136–140.

Radsak, K.D., Freise, H.W., 1972. Stimulation of mitochondrial DNA synthesis in HeLa cells by herpes simplex virus. Life Sci. II 11 (14), 717–724.

Rhim, J.S., Schell, K., Creasy, B., Case, W., 1969. Biological characteristics and viral susceptibility of an African green monkey kidney cell line (Vero). Proc. Soc. Exp. Biol. Med. 132 (2), 670–678.

Rice, S.A., Knipe, D.M., 1990. Genetic evidence for two distinct transactivation functions of the herpes simplex virus alpha protein ICP27. J. Virol. 64 (4), 1704–1715.

Rice, S.A., Long, M.C., Lam, V., Schaffer, P.A., Spencer, C.A., 1995. Herpes simplex virus immediate-early protein ICP22 is required for viral modification of host RNA polymerase II and establishment of the normal viral transcription program. J. Virol. 69 (9), 5550–5559.

Roizman, B., 1962. Polykaryocytosis induced by viruses. Proc. Natl. Acad. Sci. U.S.A. 48, 228–234.

Roizman, B., Knipe, D.M., 2001. Herpes Simplex Viruses and their Replication. In: Knipe, D.M., Howley, P.M. (Eds.), Virology, fourth ed. Lippincott-Raven, Philadelphia, PA, pp. 2399–2459.

Roizman, B., Roanne, P.R., 1964. Multiplication of herpes simplex virus: II. The relationship between protein synthesis and the duplication of viral DNA in infected HEp-2 cells. Virology 22, 262–269.

Roizman, B., Sears, A., 1996. Herpes Simplex Viruses and their Replication. In: Fields, B.N., Knipe, D.M. (Eds.), Virology, third ed. Lippincott-Raven, Philadelphia, PA, pp. 2231–2295.

Sacks, W.R., Greene, C.C., Aschman, D.P., Schaffer, P.A., 1985. Herpes simplex virus type 1 ICP27 is an essential regulatory protein. J. Virol. 55 (3), 796–805.

Salvesen, G.S., Dixit, V.M., 1997. Caspases: intracellular signaling by proteolysis. Cell 91 (4), 443–646.

Samaniego, L.A., Wu, N., DeLuca, N.A., 1997. The herpes simplex virus immediate-early protein ICP0 affects transcription from the viral genome and infected-cell survival in the absence of ICP4 and ICP27. J. Virol. 71 (6), 4614–4625.

Sanfilippo, C.M., Blaho, J.A., 2003. The facts of death. Int. Rev. Immunol. 22 (5–6), 327–340.

Sanfilippo, C.M., Chirimuuta, F.N., Blaho, J.A., 2004. Herpes simplex virus type 1 immediate-early gene expression is required for the induction of apoptosis in human epithelial HEp-2 cells. J. Virol. 78 (1), 224–239.

Soliman, T.M., Sandri-Goldin, R.M., Silverstein, S.J., 1997. Shuttling of the herpes simplex virus type 1 regulatory protein ICP27 between the nucleus and cytoplasm mediates the expression of late proteins. J. Virol. 71 (12), 9188–9197.

Vaux, D.L., Strasser, A., 1996. The molecular biology of apoptosis. Proc. Natl. Acad. Sci. U.S.A. 93 (6), 2239–2244.

Villa, P., Kaufmann, S.H., Earnshaw, W.C., 1997. Caspases and caspase inhibitors. Trends Biochem. Sci. 22 (10), 388–393.

Visalli, R.J., Brandt, C.R., 1991. The HSV-1 UL45 gene product is not required for growth in Vero cells. Virology 185 (1), 419–423.

Watson, R.J., Clements, J.B., 1980. A herpes simplex virus type 1 function continuously required for early and late virus RNA synthesis. Nature 285 (5763), 329–330.

White, E., 1996. Life, death, and the pursuit of apoptosis. Genes Dev. 10, 1–15.

White, E., 2001. Regulation of the cell cycle and apoptosis by the oncogenes of adenovirus. Oncogene 20 (54), 7836–7846.

Wilson, S.E., Pedroza, L., Beuerman, R., Hill, J.M., 1997. Herpes simplex virus type-1 infection of corneal epithelial cells induces apoptosis of the underlying keratocytes. Exp. Eye Res. 64 (5), 775–779.

Wu, N., Watkins, S.C., Schaffer, P.A., DeLuca, N.A., 1996. Prolonged gene expression and cell survival after infection by a herpes simplex virus mutant defective in the immediate-early genes encoding ICP4, ICP27, and ICP22. J. Virol. 70 (9), 6358–6369.

Wyllie, A.H., Kerr, J.F., Currie, A.R., 1980. Cell death: the significance of apoptosis. Int. Rev. Cytol. 68, 251–306.

Zachos, G., Koffa, M., Preston, C.M., Clements, J.B., Conner, J., 2001. Herpes simplex virus type 1 blocks the apoptotic host cell defense mechanisms that target Bcl-2 and manipulates activation of p38 mitogen-activated protein kinase to improve viral replication. J. Virol. 75 (6), 2710–2728.

Zheng, X., Silverman, R.H., Zhou, A., Goto, T., Kwon, B.S., Kaufman, H.E., Hill, J.M., 2001. Increased severity of HSV-1 keratitis and mortality in mice lacking the 2-5A-dependent RNase L gene. Invest. Ophthalmol. Visual Sci. 42 (1), 120–126.

Zhou, G., Roizman, B., 2000. Wild-type herpes simplex virus 1 blocks programmed cell death and release of cytochrome *c* but not the translocation of mitochondrial apoptosis-inducing factor to the nuclei of human embryonic lung fibroblasts. J. Virol. 74 (19), 9048–9053.

Zhou, G., Roizman, B., 2002. Truncated forms of glycoprotein D of herpes simplex virus 1 capable of blocking apoptosis and of low-efficiency entry into cells form a heterodimer dependent on the presence of a cysteine located in the shared transmembrane domains. J. Virol. 76 (22), 11469–11475.